Improving volcanic sulfur dioxide cloud dispersal forecasts by progressive assimilation of satellite observations

Marie Boichu, Lieven Clarisse, Dmitry Khvorostyanov, Cathy Clerbaux

AGU PUBLICATIONS

Geophysical Research Letters

RESEARCH LETTER
10.1002/2014GL059496

Key Points:
- Refined SO_2 cloud dispersal forecasts by assimilation of satellite observations
- Refined estimation of source emissions using an inverse modeling approach
- Compared to standard methods, cloud SO_2-rich parts are robustly forecasted

Supporting Information:
- Readme
- Figures S1–S5

Correspondence to:
M. Boichu,
mboichu@lmd.ens.fr

Citation:
Boichu, M., L. Clarisse, D. Khvorostyanov, and C. Clerbaux (2014), Improving volcanic sulfur dioxide cloud dispersal forecasts by progressive assimilation of satellite observations, *Geophys. Res. Lett.*, *41*, 2637–2643, doi:10.1002/2014GL059496.

Received 6 FEB 2014
Accepted 10 MAR 2014
Accepted article online 20 MAR 2014
Published online 11 APR 2014

Improving volcanic sulfur dioxide cloud dispersal forecasts by progressive assimilation of satellite observations

Marie Boichu[1], Lieven Clarisse[2], Dmitry Khvorostyanov[1], and Cathy Clerbaux[2,3]

[1]Laboratoire de Météorologie Dynamique, CNRS/INSU, École Normale Supérieure de Paris, École Polytechnique, Université Pierre et Marie Curie, UMR 8539, IPSL, Paris, France, [2]Spectroscopie de l'Atmosphère, Service de Chimie Quantique et Photophysique, Université Libre de Bruxelles, Brussels, Belgium, [3]Université Pierre et Marie Curie, Université Versailles St-Quentin, CNRS/INSU, LATMOS-IPSL, UMR8190, Paris, France

Abstract Forecasting the dispersal of volcanic clouds during an eruption is of primary importance, especially for ensuring aviation safety. As volcanic emissions are characterized by rapid variations of emission rate and height, the (generally) high level of uncertainty in the emission parameters represents a critical issue that limits the robustness of volcanic cloud dispersal forecasts. An inverse modeling scheme, combining satellite observations of the volcanic cloud with a regional chemistry-transport model, allows reconstructing this source term at high temporal resolution. We demonstrate here how a progressive assimilation of freshly acquired satellite observations, via such an inverse modeling procedure, allows for delivering robust sulfur dioxide (SO_2) cloud dispersal forecasts during the eruption. This approach provides a computationally cheap estimate of the expected location and mass loading of volcanic clouds, including the identification of SO_2-rich parts.

1. Introduction

In the event of an eruption, volcanic products can pose significant hazards to aircrafts. Ash represents the main hazard as it causes damages ranging from engine failure, windshields abrasion, and disruption of sensitive avionics equipment [*Prata*, 2009]. Sulfur dioxide (SO_2) also generates a potential danger if exposure is chronic, as sulphidation of the metals in jet turbine fans could lead to engine damage [*Carn et al.*, 2009]. Therefore, providing robust forecasts of the atmospheric evolution of the emitted ash- and gas-rich volcanic cloud, in terms of location and concentration, is crucial to reliably assess the extent of restricted flight airspace and thereby to ensure safe air travels [*Bonadonna et al.*, 2012].

On one hand, on a continental scale, numerical chemistry-transport models, forced by meteorological observations, now allow for estimating with a high degree of confidence the expected trajectory within the atmospheric circulation system of any given ash/gas parcel emitted by a volcano [e.g., *Haywood et al.*, 2010; *Heard et al.*, 2012]. Overall, SO_2 and ash are likely to follow the same trajectory if emitted at similar injection heights [e.g., *Thomas and Prata*, 2011]. As SO_2 is the most easily detected species from space, SO_2 is often taken as a convenient indicator of the likely presence of ash [*Carn et al.*, 2009; *Sears et al.*, 2013]. However, ash and SO_2 can be separated due to different production mechanisms at source or a distinct settling velocity combined with wind shear [*Schneider et al.*, 1999; *Prata and Kerkmann*, 2007]. Most importantly, volcanic ash and SO_2 release is characterized by rapid variations in both emission rate and height [*Stohl et al.*, 2011; *Boichu et al.*, 2013]. Unfortunately, most of the active volcanoes in the world are still not or poorly monitored so that our knowledge of these emission parameters remains limited [*Marzocchi et al.*, 2012]. As a consequence, the initialization of numerical simulations of atmospheric chemistry-transport and the resulting robustness of volcanic cloud dispersal forecasts are subject to large uncertainty [*Webley and Mastin*, 2009; *Bonadonna et al.*, 2012].

When local ground observations are lacking or become practically inoperative, satellite observations of volcanic clouds can be used to track the evolution of eruptive activity. Assuming that the swath of satellite observations allows fully capturing the volcanic cloud, various space-based methods have been proposed to estimate the SO_2 emission flux. The crudest approach consists in differentiating in time the SO_2 mass burdens retrieved from successive acquisitions [e.g., *Krueger et al.*, 1996; *Surono et al.*, 2012; *Lopez et al.*, 2013]. Unfortunately, this approach only provides estimates of SO_2 fluxes averaged over 12 to 24 h at best, depending on polar-orbiting satellite revisit frequency. In order to reconstruct time series of SO_2 emission fluxes at

higher temporal resolution, it is necessary to exploit the spatial variations of the SO_2 concentration within the plume. This can be achieved by integrating SO_2 column densities along a series of transects crossing the volcanic cloud and multiplying by wind speed [e.g., *Carn and Bluth*, 2003; *Merucci et al.*, 2011; *Theys et al.*, 2013]. However, this method has neither been developed nor has it been tested for operational purposes of volcanic cloud dispersal forecast, probably due to its heuristic nature.

To establish more firmly the link between in-cloud spatial heterogeneities of SO_2 concentration and temporal variability of the volcanic source, an inverse modeling approach is required, whereby satellite observations of the volcanic cloud are coupled with a chemistry-transport model. As demonstrated by *Boichu et al.* [2013], such an approach can effectively reconstruct retrospectively SO_2 flux time series with an hourly temporal resolution, without the need for a priori knowledge on the SO_2 flux.

Here we focus on the 2010 Eyjafjallajökull eruption to show that this inverse modeling approach provides more robust forecasts of the volcanic SO_2 cloud spatial extent and mass loading than regular mass-burden methods. When applied progressively to a set of satellite observations of the volcanic cloud acquired at regular time intervals during the course of an eruption, the reconstruction of the source term can be updated to provide refined forecasts for the next 12–36 h.

2. Methodology

The atmospheric evolution of the volcanic cloud is described using the CHIMERE regional Eulerian chemistry-transport model [*Menut et al.*, 2013; *Boichu et al.*, 2013], driven by Global Forecasting System-Weather Research and Forecasting model reanalysis meteorological fields [*Skamarock et al.*, 2008], with a 25 km × 25 km horizontal grid (for both meteorological and chemistry-transport models) and 18 hybrid sigma-pressure vertical layers extending up to 200 hPa (~12 km above sea level (asl)). Previous inverse modeling studies have focused on the retrieval of the emission profile with altitude, assuming a constant volcanic flux emitted on a short time span [*Eckhardt et al.*, 2008; *Kristiansen et al.*, 2010]. In our study, emission height is constrained by independent observations. SO_2 emissions are released along a 1 km full width at half maximum semi-Gaussian profile centered at a height of 6 km asl, in agreement with radar and web camera observations of the Eyjafjallajökull plume [*Petersen et al.*, 2012]. As shown by *Boichu et al.* [2013], removal mechanisms of SO_2 can be neglected in the early May period of the eruption.

SO_2 column amount maps were retrieved from measurements of the polar-orbiting Infrared Atmospheric Sounding Interferometer (IASI) sounder, which provides global coverage twice a day (mean overpass times at 09:30 and 21:30 local time) with a pixel size of 12 km at nadir. For simplicity and in the absence of independent observations, a constant altitude of the volcanic cloud is assumed and fixed to 7 km asl, close to emission height, in the retrieval algorithm. For more details, the reader is referred to *Boichu et al.* [2013].

Two different emission terms are tested for initializing plume chemistry-transport modeling, consisting in time series of the SO_2 flux reconstructed until a chosen date t_0 either by the standard mass-burden method (Method 1) or by a multiple-image inversion scheme (Method 2), both procedures capitalizing on the series of satellite observations acquired until t_0. Method 1 consists in differentiating the SO_2 burdens from two consecutive images of the volcanic cloud to evaluate a mean SO_2 flux, assuming negligible SO_2 depletion in the volcanic cloud [e.g., *Surono et al.*, 2012; *Lopez et al.*, 2013; *Theys et al.*, 2013]. Method 2 is an inversion procedure that uses the satellite observations in combination with the chemistry-transport model as a forward model [*Boichu et al.*, 2013]. The inverse problem is solved by determining the time history of the SO_2 flux that minimizes (in the least squares sense) the misfit between observed and modeled spatial and temporal distributions of SO_2 within one or several images. Except for a nonnegative constraint, no a priori knowledge on the SO_2 flux is required in this inversion procedure. To tackle numerical diffusion biases, the set of pixels corresponding to a mass load below the detection threshold (null detection) is decimated by a factor 10, and a weak smoothing of the SO_2 flux solution is applied. Details on this inversion scheme are provided in *Boichu et al.* [2013].

To demonstrate how the forecast can be progressively updated and improved during the course of the eruption, we apply this assimilation procedure to either a single satellite image or sequentially to a set of several successive freshly acquired images, hereafter referred to as "progressive assimilation." Given a revisit time of IASI less than or equal to $\Delta T = 12$ h at any specific location, forecasts are consequently computed with the same periodicity. In the absence of observations constraining the emissions between t_0 and the forecast

time $t_0 + \Delta t$, we assume that the volcano flux $\Phi(t)$ proceeds at a constant rate $\Phi_{t_0,\tau}$ equal to the mean of the reconstructed flux values over a period τ preceding the last detection of the volcanic cloud in the t_0 image:

$$\forall t \in [t_0; t_0 + \Delta t],\ \Phi(t) = \Phi_{t_0,\tau} = \frac{1}{\tau}\int_{t_0-\tau}^{t_0} \Phi(t')\mathrm{d}t' \quad (1)$$

Here τ has been arbitrarily set to 6 h.

So far, there is no consensus on the choice of a standard metric to quantitatively estimate the agreement between modeled and observed volcanic cloud dispersion. Here the improvement of forecasts achieved by progressive assimilation of satellite observations is assessed using the Earth Mover's Distance (EMD) metric, which is commonly used in many applications of computer vision including image retrieval and detection of similar features [*Rubner et al.*, 2000; *Pele and Werman*, 2009; *Collins and Ge*, 2008]. The EMD quantifies the minimal cost that must be paid to transform one distribution (here the SO_2 mass loading value for each pixel) into the other. Compared to the simpler root-mean-square error, the EMD is not dominated by biases induced by numerical diffusion issues, which makes it more adapted to rank the similarity between a reference image (the observation) and two candidate images (the output of two different forecasts).

3. Forecast Initialization by Mass Burden Versus Inversion-Derived Flux

After a few days of relative quiescence, early May 2010 corresponds to a phase of renewal of the explosive activity at Eyjafjallajökull volcano [*Gudmundsson et al.*, 2012], which is accompanied by an intense degassing of SO_2 captured by ultraviolet and infrared satellite sensors [*Thomas and Prata*, 2011; *Carboni et al.*, 2012; *Rix et al.*, 2012; *Boichu et al.*, 2013]. Figure 1 illustrates the comparison of simulation maps (centered at the date t_0 = 7 May 12:00 UTC) and forecast maps (centered at $t_0+\Delta T$ = 8 May 00:00 UTC) of the Eyjafjallajökull SO_2 cloud dispersal. Forecasts are initialized using source terms obtained from Methods 1 and 2 (Figure 1d), both using the IASI observations of the Eyjafjallajökull cloud available before the date t_0.

Geographical location and spatial extent of the modeled SO_2 cloud at t_0 are in overall agreement with IASI observations, whichever the method applied to determine the source term. The correct location of the modeled SO_2 cloud, mainly aligned toward Greenland at t_0, then also extending toward Spain at $t_0+\Delta T$, indicates the robustness of the meteorological field that forces the chemistry-transport model. However, only the forecast initialized using Method 2 is able to correctly reproduce the spatial variability of the SO_2 cloud concentration (Figure 1c2). In agreement with IASI observations, three local peaks of SO_2 are distinguished and the volcanic cloud is split into essentially two separated parts, whereas the forecast initialized using Method 1 (Figure 1b2) misses completely the dense and elongated peak 2 and predicts a one-piece SO_2 cloud. The latter method also underestimates the elongation of peak 1 and the mass loading of peak 3. The reason for this poor performance is that the mass-burden method only provides an average representation of the emissions, in the form of a step function (Figure 1d, red line), which smoothes any high-frequency variation of the actual SO_2 flux. As a consequence, the resulting simulation and forecast cannot reproduce all of the heterogeneities of concentration within the SO_2 cloud and, most importantly, may miss the parts of the volcanic cloud with the richest SO_2 mass loadings which are correctly captured by Method 2.

4. SO_2 Cloud Dispersal Forecast Improvement by Progressive Assimilation of Satellite Observations

Figures 2 and S1–S5 in the supporting information demonstrate, through the study of 20 forecast cases, how the progressive assimilation of the satellite observations available during the course of an eruption provides a refined (high temporal resolution) estimate of the source term which improves the robustness of short-term forecasts. Considering that the first IASI satellite measurement of the Eyjafjallajökull SO_2 cloud is available at t_0 (t_0 = 8 May 00:00 UTC in Figure 2) and that the revisit time of IASI is anywhere less than or equal to ΔT = 12 h, we compute a series of forecasts at $t_0+\Delta T$, $t_0+2\Delta T$, and $t_0+3\Delta T$, initialized with the source term reconstructed from the inversion of the single t_0 image (Figure 2b). This latter single-image-based forecast at $t_0+3\Delta T$ (Figure 2b4) is then compared with the forecasts initialized with the source term derived from a two-image (i.e., using t_0 and $t_0+\Delta T$ images, Figure 2c4) or three-image inversions (i.e., using t_0, $t_0+\Delta T$, and $t_0+2\Delta T$ images, Figure 2d4). The comparison of these forecasts with actual

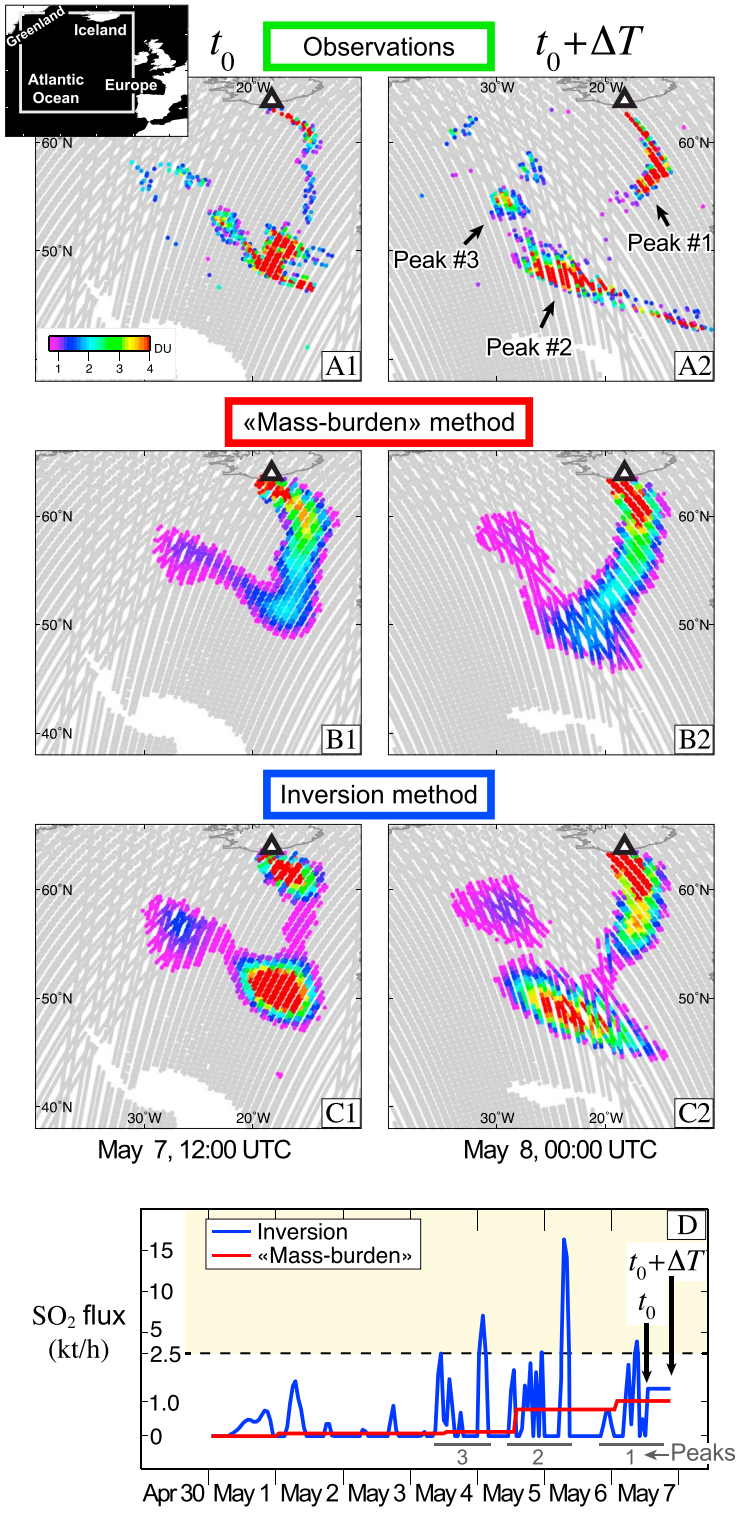

Figure 1. Forecasts initialized using source terms derived either from the standard mass-burden method (Method 1) or from the multiple-image inversion scheme (Method 2). (a) IASI satellite retrievals (Dobson unit (DU)) of the Eyjafjallajökull SO_2 cloud. (b1) Simulation at t_0 (7 May 12:00 UTC) and (b2) forecast at $t_0+\Delta T$ (8 May 00:00 UTC) initialized by the (d) SO_2 flux derived from the mass-burden method (red line). (c1) Simulation and (c2) forecast initialized by the SO_2 flux derived from the inversion scheme (Figure 1d, blue line). Modeled maps are collocated (in time and space) with IASI observations acquired over a 12 h window centered at the time t_0 or $t_0+\Delta T$. Regions in grey indicate column amounts less than 0.7 DU (detection threshold in IASI processing). Black triangle indicates Eyjafjallajökull volcano. Note the change in vertical scale in Figure 1d for flux > 2.5 kt h^{-1}.

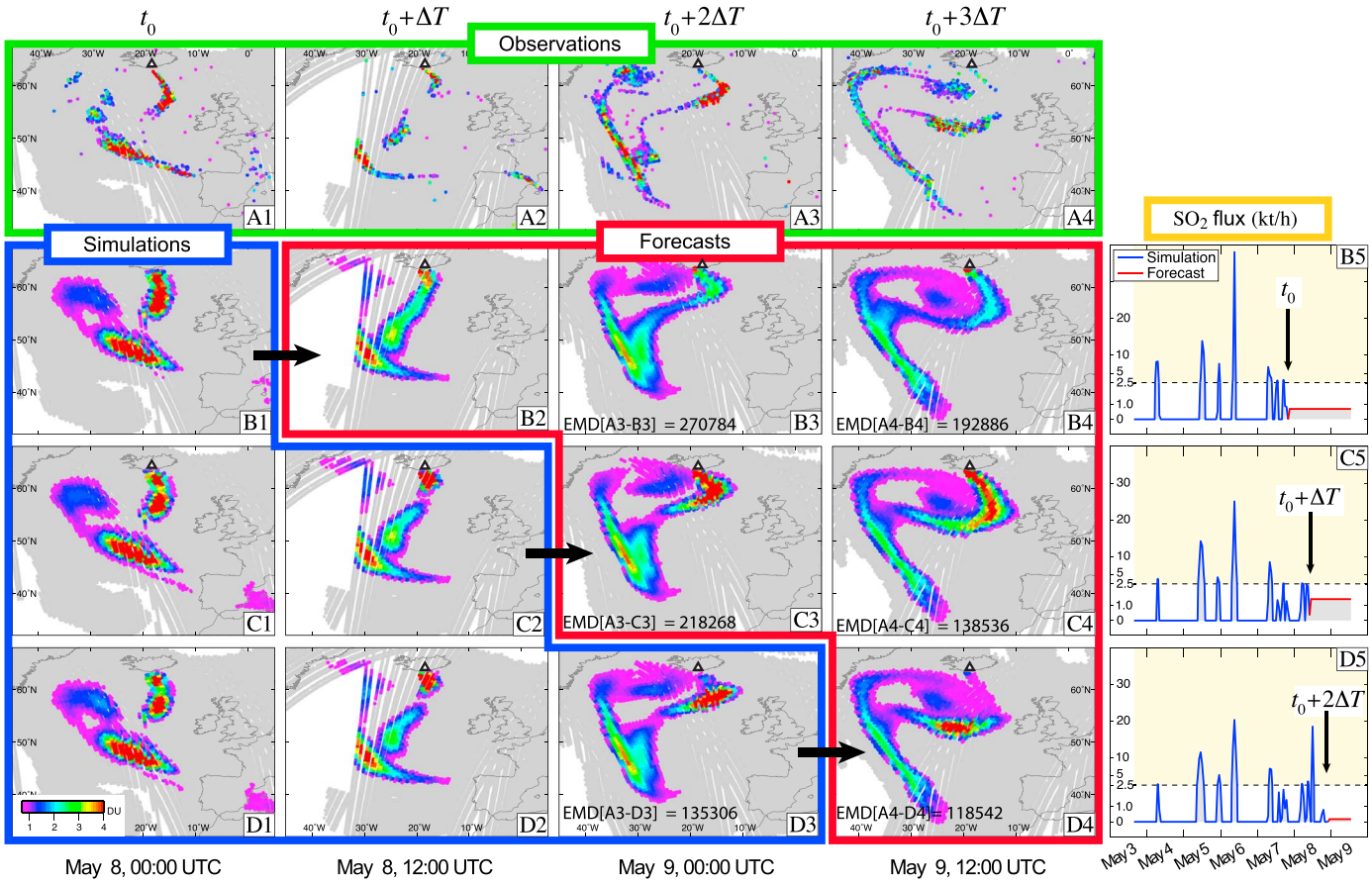

Figure 2. Forecast improvement by progressive assimilation of SO_2 cloud satellite observations. (a) IASI SO_2 observations (green) acquired during the course of the Eyjafjallajökull eruption. Simulation (blue) or forecast (red) maps of the SO_2 cloud dispersal at (1) t_0 (8 May 00:00 UTC), (2) $t_0+\Delta T$, (3) $t_0+2\Delta T$, and (4) $t_0+3\Delta T$ (ΔT = 12 h). Simulations and forecasts are initialized using SO_2 flux time series derived from the inversion of (b) the single t_0 image; (c) t_0 and ($t_0+\Delta T$) images; and (d) t_0, ($t_0+\Delta T$), and ($t_0+2\Delta T$) images. Corresponding SO_2 flux time series are shown on the right (note the change in vertical scaling above 2.5 kt h^{-1}). Earth Mover's Distance (EMD) between forecast and satellite retrievals at a given date are indicated. For comparison, EMD between a map filled with zero values and satellite data at $t_0+2\Delta T$ and $t_0+3\Delta T$ are drastically higher (equal to 690,000 and 498,000, respectively).

IASI observations made at $t_0+3\Delta T$ (Figure 2a4) shows that the source derived from the three-image inversion provides the best forecast, as illustrated by the lowest EMD value indicative of strongest similarity (Figure 2d4). This best forecast is the only one that reproduces correctly the spatial variations of SO_2 concentration in the Eyjafjallajökull cloud and, most importantly, that successfully identifies the location and extent of the densest SO_2 part of the volcanic cloud. This most SO_2-concentrated zone is less well positioned with the sources derived from the one- or two-image inversions (Figures 2b4 and 2c4). An improvement of ~ 40%, in terms of similarity or EMD decrease, is achieved relative to the single-image-based forecast. Following the same rationale, the source derived from the two-image inversion provides the forecast (Figure 2c3) which best matches observations at $t_0+2\Delta T$ (Figure 2a3), as confirmed by an EMD value weaker by ~ 20% relative to the single-image-based forecast (Figure 2b3). Additional time series in Figures S1–S5 illustrate the systematic improvement of forecasts (one case excepted) by assimilation of the last acquired image, which is corroborated by a consistent decrease of EMD between 5 and 43% relatively to forecasts derived from single-image inversion.

5. Discussion

The inversion procedure introduces a feedback loop between satellite observations of the volcanic cloud and the atmospheric chemistry-transport model. As demonstrated in the above analysis, this procedure leads to a significant improvement of the temporal resolution on the source term and a consequent improvement in the spatial accuracy of the SO_2 cloud dispersal forecasts. Furthermore, this approach is more

robust than the standard mass-burden procedure, in the sense that it has a lower tendency to map errors in the observations or the modeling scheme into errors in the forecast.

For instance, forecasts initialized with both mass-burden and inversion-derived source methods suffer from numerical diffusion issues that are inherent to Eulerian chemistry-transport models [*Freitas et al.*, 2012; *Boichu et al.*, 2013]. This results in an overestimation of the SO_2 dispersion that increases as the volcanic cloud gets older and travels farther from its source (Figure 1). This modeling bias inevitably leads to an underestimation of the modeled SO_2 cloud mass loading and an overestimation of the SO_2 spreading (Figure 1). Nevertheless, the image inversion procedure allows for partly counterbalancing this bias by boosting the amplitude of the reconstructed SO_2 flux, which therefore attenuates SO_2 cloud mass loading underestimation, in order to achieve a better fit to satellite retrievals.

Another advantage of the multiple-image inversion procedure is that it is robust against gaps in satellite retrievals, which often occur due to interruptions in satellite data transmission (as illustrated in Figure 2a2) or because of the presence of thick meteorological clouds absorbing infrared radiation and masking any underlying SO_2. Whereas such data gaps inevitably lead to a (potentially significant) underestimation of emission rates with the mass-burden method, their impact is mitigated using the multiple-image inversion procedure which incorporates redundant observations of the same parcel of SO_2 at different ages, in cloudy but also in noncloudy scenes.

Emission height impacts the volcanic cloud trajectory but also SO_2 lifetime. When little wind shear is recorded throughout the full plume, as during the May 2010 Eyjafjallajökull eruption, SO_2 cloud dispersal simulations are weakly dependent on the uncertainty on emission height [*Boichu et al.*, 2013; *Flemming and Inness*, 2013]. However, in case of significant wind shear, assuming an inaccurate plume top height may lead to dramatic errors on SO_2 cloud dispersal forecasts. Fortunately, in such cases, emission height can be estimated from back trajectory analysis [*Eckhardt et al.*, 2008; *Kristiansen et al.*, 2010; *Hughes et al.*, 2012]. Introducing the emission altitude as an additional source parameter to reconstruct in our inverse modeling scheme would be straightforward. However, this would lead to a significant increase of the computational time for two reasons. First, a supplementary degree of freedom has to be introduced in the inversion procedure, thereby increasing the number of linear equations involved in the inverse problem. Moreover, a refinement of the vertical grid spacing in the chemistry-transport model would be required to fully capture the vertical dynamics of the plume.

Applied to SO_2 volcanic clouds, the assimilation scheme presented here could be extended to the monitoring of ash-rich clouds. This low-cost procedure, which strengthens feedback between observations and model, could be automated for operational application, so as to provide better-resolved forecasts of volcanic cloud dispersal.

Acknowledgments

M. Boichu and D. Khvorostyanov gratefully acknowledge support from the French ANR-funded CHEDAR project. IASI has been developed and built under the responsibility of the Centre National d'Etudes Spatiales (CNES, France). It is flown on board the Metop satellites as part of the EUMETSAT Polar System. The IASI L1 data are received through the EUMETCast near-real-time data distribution service. L. Clarisse is a postdoctoral researcher (Chargé de Recherches) with F.R.S.-FNRS. C. Clerbaux is grateful to CNES for scientific collaboration and financial support. The research in Belgium was funded by the F.R.S.-FNRS (M.I.S. nF.4511.08), the Belgian State Federal Office for Scientific, Technical and Cultural Affairs, and the European Space Agency (ESA-Prodex arrangements and the Support to Aviation Control Service (SACS2) project). The authors acknowledge the two anonymous reviewers for their insightful reviews which helped to improve the quality of the manuscript.

The Editor thanks Larry Mastin and Peter Webley for their assistance in evaluating this paper.

References

Boichu, M., L. Menut, D. Khvorostyanov, L. Clarisse, C. Clerbaux, S. Turquety, and P.-F. Coheur (2013), Inverting for volcanic SO_2 flux at high temporal resolution using spaceborne plume imagery and chemistry-transport modelling: The 2010 Eyjafjallajökull eruption case study, *Atmosph. Chem. Phys.*, *13*(17), 8569–8584, doi:10.5194/acp-13-8569-2013.

Bonadonna, C., A. Folch, S. Loughlin, and H. Puempel (2012), Future developments in modelling and monitoring of volcanic ash clouds: Outcomes from the first IAVCEI-WMO workshop on Ash Dispersal Forecast and Civil Aviation, *Bull. Volcanol.*, *74*, 1–10, doi:10.1007/s00445-011-0508-6.

Carboni, E., R. Grainger, J. Walker, A. Dudhia, and R. Siddans (2012), A new scheme for sulphur dioxide retrieval from IASI measurements: Application to the Eyjafjallajökull eruption of April and May 2010, *Atmosph. Chem. Phys.*, *12*(23), 11,417–11,434.

Carn, S., A. Krueger, N. Krotkov, K. Yang, and K. Evans (2009), Tracking volcanic sulfur dioxide clouds for aviation hazard mitigation, *Nat. Hazards*, *51*, 325–343, doi:10.1007/s11069-008-9228-4.

Carn, S. A., and G. J. S. Bluth (2003), Prodigious sulfur dioxide emissions from Nyamuragira volcano, DR Congo, *Geophys. Res. Lett.*, *30*(23), 2211, doi:10.1029/2003GL018465.

Collins, R. T., and W. Ge (2008), CSDD features: Center-Surround Distribution Distance for feature extraction and matching, in *ECCV '08 Proceedings of the 10th European Conference on Computer Vision: Part III*, pp. 140–153, Springer-Verlag, Berlin, Heidelberg.

Eckhardt, S., A. J. Prata, P. Seibert, K. Stebel, and A. Stohl (2008), Estimation of the vertical profile of sulfur dioxide injection into the atmosphere by a volcanic eruption using satellite column measurements and inverse transport modeling, *Atmosph. Chem. Phys.*, *8*, 3881–3897.

Flemming, J., and A. Inness (2013), Volcanic sulfur dioxide plume forecasts based on UV satellite retrievals for the 2011 Grimsvötn and the 2010 Eyjafjallajökull eruption, *J. Geophys. Res. Atmos.*, *118*, 10,172–10,189, doi:10.1002/jgrd.50753.

Freitas, S., L. F. Rodrigues, K. M. Longo, and J. Panetta (2012), Impact of a monotonic advection scheme with low numerical diffusion on transport modeling of emissions from biomass burning, *J. Adv. Model. Earth Syst.*, *4*, M01001, doi:10.1029/2011MS000084.

Gudmundsson, M., et al. (2012), Ash generation and distribution from the April–May 2010 eruption of Eyjafjallajökull, Iceland, *Sci. Rep.*, *2*, 572, doi:10.1038/srep00572.

Haywood, J. M., et al. (2010), Observations of the eruption of the Sarychev volcano and simulations using the HadGEM2 climate model, *J. Geophys. Res.*, *115*, D21212, doi:10.1029/2010JD014447.

Heard, I. P. C., A. J. Manning, J. M. Haywood, C. Witham, A. Redington, A. Jones, L. Clarisse, and A. Bourassa (2012), A comparison of atmospheric dispersion model predictions with observations of SO_2 and sulphate aerosol from volcanic eruptions, *J. Geophys. Res.*, *117*, D00U22, doi:10.1029/2011JD016791.

Hughes, E., L. Sparling, S. Carn, and A. Krueger (2012), Using horizontal transport characteristics to infer an emission height time series of volcanic SO_2, *J. Geophys. Res.*, *117*, D18307, doi:10.1029/2012JD017957.

Kristiansen, N., et al. (2010), Remote sensing and inverse transport modeling of the Kasatochi eruption sulfur dioxide cloud, *J. Geophys. Res.*, *115*, D00L16, doi:10.1029/2009JD013286.

Krueger, A., C. Schnetzler, and L. Walter (1996), The December 1981 eruption of Nyamuragira volcano (Zaire), and the origin of the "mystery cloud" of early 1982, *J. Geophys. Res.*, *101*(D10), 15,191–15,196.

Lopez, T., S. Carn, C. Werner, D. Fee, P. Kelly, M. Doukas, M. Pfeffer, P. Webley, C. Cahill, and D. Schneider (2013), Evaluation of Redoubt Volcano's sulfur dioxide emissions by the Ozone Monitoring Instrument, *J. Volcanol. Geoth. Res.*, *259*, 290–307, doi:10.1016/j.jvolgeores.2012.03.002.

Marzocchi, W., C. Newhall, and G. Woo (2012), The scientific management of volcanic crises, *J. Volcanol. Geoth. Res.*, 181–189.

Menut, L., et al. (2013), Regional atmospheric composition modeling with CHIMERE, *Geosci. Model Dev.*, *6*, 981–1028, doi:10.5194/gmd-6-981-2013.

Merucci, L., M. Burton, S. Corradini, and G. G. Salerno (2011), Reconstruction of SO_2 flux emission chronology from space-based measurements, *J. Volcanol. Geoth. Res.*, *206*, 80–87, doi:10.1016/j.jvolgeores.2011.07.002.

Pele, O., and M. Werman (2009), Fast and robust Earth Mover's Distances, in *IEEE 12th International Conference on Computer Vision*, pp. 460–467, IEEE, Kyoto, Japan.

Petersen, G. N., H. Bjornsson, and P. Arasonl (2012), The impact of the atmosphere on the Eyjafjallajökull 2010 eruption plume, *J. Geophys. Res.*, *117*, D00U07, doi:10.1029/2011JD016762.

Prata, A. (2009), Satellite detection of hazardous volcanic clouds and the risk to global air traffic, *Nat. Hazards*, *51*, 303–324, doi:10.1007/s11069-008-9273-z.

Prata, A. J., and J. Kerkmann (2007), Simultaneous retrieval of volcanic ash and SO_2 using MSG-SEVIRI measurements, *Geophys. Res. Lett.*, *34*, L05813, doi:10.1029/2006GL028691.

Rix, M., P. Valks, N. Hao, D. Loyola, H. Schlager, H. Huntrieser, J. Flemming, U. Koehler, U. Schumann, and A. Inness (2012), Volcanic SO_2, BrO and plume height estimations using GOME-2 satellite measurements during the eruption of Eyjafjallajökull in May 2010, *J. Geophys. Res.*, *117*, D00U19, doi:10.1029/2011JD016718.

Rubner, Y., C. Tomasi, and L. J. Guibas (2000), The Earth Mover's Distance as a metric for image retrieval, *Int. J. Comput. Vision*, *40*(2), 99–121.

Schneider, D. J., W. I. Rose, L. R. Coke, G. J. Bluth, I. E. Sprod, and A. J. Krueger (1999), Early evolution of a stratospheric volcanic eruption cloud as observed with TOMS and AVHRR, *J. Geophys. Res.*, *104*(D4), 4037–4050.

Sears, T., G. Thomas, E. Carboni, A. Smith, and R. Grainger (2013), SO_2 as a possible proxy for volcanic ash in aviation hazard avoidance, *J. Geophys. Res. Atmos.*, *118*, 1–12, doi:10.1002/jgrd.50505.

Skamarock, J., W. Klemp, J. Dudhia, D. Gill, D. Barker, M. Duda, X. Huang, W. Wang, and J. Powers (2008), A description of the advanced research WRF version 3, *Tech. Note NCAR/TN–475+ STR.*, Natl. Cent. for Atmos. Res., Boulder, Colo.

Stohl, A., et al. (2011), Determination of time- and height-resolved volcanic ash emissions and their use for quantitative ash dispersion modeling: The 2010 Eyjafjallajökull eruption, *Atmosph. Chem. Phys.*, *11*, 4333–4351, doi:10.5194/acp-11-4333-2011.

Surono, J. P., et al. (2012), The 2010 explosive eruption of Java's Merapi volcano—A "100-year" event, *J. Volcanol. Geoth. Res.*, *241-242*, 121–135, doi:10.1016/j.jvolgeores.2012.06.018.

Theys, N., et al. (2013), Volcanic SO_2 fluxes derived from satellite data: A survey using OMI, GOME-2, IASI and MODIS, *Atmos. Chem. Phys.*, *13*(12), 5945–5968, doi:10.5194/acp-13-5945-2013.

Thomas, H. E., and A. J. Prata (2011), Sulphur dioxide as a volcanic ash proxy during the April–May 2010 eruption of Eyjafjallajökull Volcano, Iceland, *Atmos. Chem. Phys.*, *11*, 6871–6880, doi:10.5194/acp-11-6871-2011.

Webley, P., and L. Mastin (2009), Improved prediction and tracking of volcanic ash clouds, *J. Volcanol. Geoth. Res.*, *186*, 1–9, doi:10.1016/j.jvolgeores.2008.10.022.